Renewable and Sustainable Energy Reviews 203 (2024) 114778

Contents lists available at ScienceDirect

Renewable and Sustainable Energy Reviews

journal homepage: www.elsevier.com/locate/rser

China's onshore wind energy potential in the context of climate change

Ling Ji [a,*], Jiahui Li [a], Lijian Sun [b], Shuai Wang [c], Junhong Guo [d], Yulei Xie [e], Xander Wang [f,**]

[a] School of Economics and Management, Beijing University of Technology, Beijing, 100124, China
[b] Chinese Academy of Surveying and Mapping, Beijing, 100830, China
[c] Goldwind Science & Technology Co., Ltd., Beijing, 100176, China
[d] College of Environmental Science and Engineering, North China Electric Power University, Beijing, 510006, China
[e] Institute of Environmental and Ecological Engineering, Guangdong University of Technology, Guangzhou, Guangdong, 510006, China
[f] School of Climate Change and Adaptation, University of Prince Edward Island, Charlottetown, PE C1A 4P3, Canada

ARTICLE INFO

Keywords:
Wind energy
Climate change
Land suitability
Potential assessment
Spatial and temporal variability

ABSTRACT

China has great potential for developing renewable energy to achieve its carbon neutrality goals. Orderly development of renewable energy is essential to enhance resource utilization efficiency and ensure safety during the energy system transition process. This study presents a thorough assessment of China's onshore wind power potential by considering the land suitability, the potential and temporal characteristics, and the impacts of climate change. The high-resolution maps combining wind resources with land conditions and climate scenarios are produced to provide insights into system planning, grid integration, and flexibility management. The results show that the capacity potential of onshore wind energy in China is 9.6 TW with an annual generation of 12.6 PWh, and 83 % of total capacity has a cost advantage with the levelized cost lower than the 60 $/MWh threshold. By comprehensively considering geographical, economic, and social criteria, around 8.1 % of the national territorial area is identified as the most suitable area for wind power development, primarily in Inner Mongolia and Xinjiang. The annual electricity generation from these areas can fulfill nearly 69 % of the nation's electricity demand. Future climate change projections indicate a remarkable generalized drop by 18 % in the north and a slight increase by 7 % in the south under the RCP 8.5 scenario. However, significant changes in wind resources are mostly within restricted areas, suggesting that future climate change would like to bring negative but limited impacts on wind power production in China.

Nomenclature	
Abbreviation	
AHP	Analytic hierarchy process
CMIP	Coupled Model Intercomparison Project
GCMs	General circulation models
LCOE	Levelized cost of energy
MCDM	Muti-criteria decision-making
RCoV	Relative coefficient of variation
RCPs	Representative concentration pathways
SSPs	Shared Socioeconomic Pathways
WPD	Wind power density
Notation	
α	wind shear exponent
c_j	a binary variable, if the cell belongs to restricted factor j, c_j is 0; otherwise, c_j is 1
EL	he episode length of wind energy
EP	the generated electricity

(*continued on next column*)

(*continued*)

I	initial construction cost
k_i	the score for criteria i
LF	lifetime of the technology
LL	the lulls of wind energy
LSI	land-use suitability index
OM	operation and maintenance cost
P_r	the rated power of wind turbine
r	the discount rate
T	the number of hours in the period
T_R	the duration of ramp events
v_c	cut-in wind speed
v_f	cut-out wind speed
v_m	observed wind speed
v_r	rated wind speed
v_w	wind speed at the hub height
w_i	weight of criteria

(*continued on next page*)

* Corresponding author.
** Corresponding author.
E-mail addresses: hdjiling@bjut.edu.cn (L. Ji), xxwang@upei.ca (X. Wang).

https://doi.org/10.1016/j.rser.2024.114778
Received 10 March 2024; Received in revised form 3 July 2024; Accepted 17 July 2024
Available online 29 July 2024
1364-0321/

(continued)

ρ	air density
λ	the duty ratio of ramp events

1. Introduction

In 2022, China's total energy consumption reached 159.39 EJ, solidifying its position as the foremost primary energy consumer [1]. A significant transition in power systems from conventional fossil fuels to renewable energy sources is an essential way to address the contradictions of energy security and socio-economic development. Due to technological advancements, sustained price reductions, and large-scale deployment capacity, wind and solar are the most competitive forms of renewable energy. By the end of 2022, wind and solar power capacity in China were 365.4 GW and 392.6 GW respectively. The proportion of both accounts for 30 % of the national installed capacity [2]. However, the corresponding power generation accounts for only 13.6 % of the total [3]. The Chinese government will further enhance the utilization of wind and solar energy to ensure energy security and achieve the 2060 carbon neutrality goal.

Existing studies suggest that China has great potential in renewable energy to facilitate the zero-carbon transformation of the power system, while the practical development of wind and solar energy is intricate. The planning and construction of wind farms should consider various factors, including geographical and meteorological conditions, as well as existing infrastructure. China's vast land area, totaling 9.6 million km^2 and divided into six climate zones and a plateau climate zone, provides abundant wind resources with significant regional variations due to its complex terrain. Among these factors, meteorological conditions, especially wind resources, play a crucial role in making optimal strategic decisions for the deployment of wind power. In the context of climate change, future fluctuations in wind speed may have potential impacts on optimal strategic deployment. Moreover, regarding the important role of land resources in ecology, food security, social and economic activities, and the human living environment, it is crucial to systematically and moderately identify the most suitable land for the development and utilization of wind resources. Studying the impacts of climate change on wind speed, evaluating wind resource potential, and assessing land suitability separately fall short of providing a comprehensive decision-making perspective for the national strategic planning of wind resource development and utilization in the face of climate change. Consequently, a high-resolution potential and temporal characteristic assessment of wind energy combining land-use suitability considerations and future climate change scenarios is desired.

2. Literature review

This section provides an overview of wind energy potential evaluation, suitable location assessment for wind farms, and wind resource variations under climate change. In addition, a specific review is presented to report the updated information on wind energy potential assessment in China.

2.1. Wind energy potential and suitable locations

A thorough potential evaluation and feasibility assessment of wind power is crucial for both policymakers and investors. Several studies were carried out to assess wind energy potential at the global [4], national [5], region [6], province [7], and island scale [8]. In some early studies, wind energy potential was roughly assessed by only considering a threshold for the resource intensity (wind power density less than 200 W/m^2 or wind speed less than 5 m/s). However, except for the wind resource conditions, technological advances, geographical conditions, and ecological environment constraints also exert significant impacts on the real potential of wind energy by considering economic feasibility and sustainable development. Technological advancements have enabled wind turbines to operate in areas with lower resource intensity and enhanced efficiency, exemplified by increased hub height and rotor diameter. Land cover is also a major factor influencing the site selection of wind farms. The supply cost of wind power is a key indicator to determine whether it is economically feasible to build wind farms, and it has been reported that there is obvious spatial heterogeneity due to various meteorological conditions and land use. Neglecting these factors typically leads to an overestimation of wind resources. Lately, increasing work has focused on the geographic, technical, and economic potential of wind power. These findings contribute to a more thorough potential analysis, elucidating the constraints on the availability of wind resources. For example, Jung et al. [9] estimated both the meteorological and technical potential of wind energy under six installation scenarios at the national and global scale. Jain et al. [5] conducted a geographical and techno-economic assessment of the solar and wind power potential in India. Enevoldsen et al. [10] reported that, when accounting for socio-technical constraints, 54 % of the total European area is limited to new onshore wind development. Mattar and Guzmán-Ibarra [11] investigated the offshore wind energy potential in Chile, assessing both its technical and economic feasibility. They computed various economic indicators, such as the net present value, internal rate of return, levelized cost of energy, and payback time. Nevertheless, when assessing the potential of wind energy, the inherent uncertainty should never be ignored, which is sourced from the adopted weather database, land utilization, and wind turbine configuration [12]. Rinne [13] stated that wind turbine technology and land use are the most significant assumptions affecting the potential estimation.

The majority of studies indicate that the available wind resources significantly surpass both present and projected future energy consumption levels [14]. Therefore, choosing suitable locations for wind farms is essential to achieve sustainable development of wind energy. Multi-criteria decision analysis approach combining the GIS tool has been seen as an effective method to evaluate suitable locations, by providing a visible suitability map [15]. Under the framework of multi-criteria decision analysis, a series of incompatible criteria are considered for selecting the optimal site of the wind farm, usually including technical, environmental, economic, and geographical standards [16]. In this process, the weighting of indicators is a crucial factor influencing the decision. The analytic hierarchy process (AHP) method has been widely applied for determining the weight of criteria due to its comprehensible logic and rapid implementation [17]. Alternative methods such as the best-worst method [16], the technique for order preference by similarity to the ideal solution [18], and VIsekriterijumsko KOmpromisno Rangiranje [15] have been employed in some studies.

2.2. Wind resource variations under climate change

Due to ongoing anthropogenic greenhouse gas emissions altering atmospheric circulation and the global climate, considerable focus has been placed on assessing the potential influences of climate change on renewable energy resources [19]. Climate models, mainly the general circulation models (GCMs) and statistically downscaled output from several GCMs, are employed to examine the effects of climate change on both wind resources and the generation of wind power [20]. The projection results are influenced by the assumptions used in climate modeling, for example, the boundary conditions, and the scenarios of climate change. Climate modeling and projecting specific variables pose challenges due to inherent uncertainties and potential errors from sources. Some work used an ensemble of several climate model simulations attempted to improve the performance. For example, according to future climate projections from Coupled Model Intercomparison Project 5 (CMIP5), Carvalho et al. [21] investigated the potential changes in wind energy resources in Europe by quantifying the anticipated alterations in the wind energy density index and its intra- and inter-annual variability. In more recent studies, the Shared

Socioeconomic Pathways (SSPs), which are complex socio-economic scenarios used in the CMIP6 program, have gained great concern. Russo et al. [22] assessed the impacts of climate change on the availability and variability of wind and solar energy in Portugal, where two climate change scenarios, SSP2-4.5 and SSP5-8.5, were compared with a present scenario. He et al. [23] investigated the future variation of wind resources in Hong Kong by using the GCMs from CMIP6 and also chose SSP2-4.5 and SSP5-8.5 to represent the future scenarios. Except for the wind resources and wind power density, some work further investigated how climate change can affect operating margins and investment values [20,24].

2.3. Case studies in China

So far, several studies have conducted wind resource potential assessments in China nationwide, including onshore, offshore, or both. These studies consider different levels of potential, turbine heights, land constraint conditions, data sources, and spatial resolutions. For example, Hong and Möller [25] investigated the technical, spatial, and economic potential of offshore wind energy resources in China's exclusive economic zone, utilizing wind data from QuikSCAT ocean wind L2B12. He and Kammen [26] evaluated the wind resources (including both onshore and offshore) at the provincial-scale for China, utilizing a decade of hourly wind speed data collected from 200 sites. In a more recent publication [27], the evaluation of onshore and offshore wind resources in China was conducted based on high spatial-temporal resolution climate data and the characteristics of mainstream wind turbines. In recent studies, some work began to concern climate change and its influences on wind resources and wind power. For example, by ensembling 8 simulations from the CORDEX project, Costoya et al. [28] predicted the future offshore wind energy resource under the RCP8.5 scenario. Based on the weighted ensembling of eleven regional climate models, Chen et al. [29] projected the variations in wind resources across China's mainland for the middle of the century under the RCP8.5 scenario. Miao et al. [30] investigated the wind energy resources change over the Northern Hemisphere. It focused on the comparison of wind speed in CMIP5 and CMIP6 models in Europe, Asia, and North America under four typical emission scenarios, SSP1-2.6, SSP2-4.5, SSP 3–7.0, and SSP5-8.5. The results showed that the wind speeds over most of China drop significantly under SSP3-7.0, while the decline is merely in the western region under the SSP5-8.5 scenario. Similarly, Wu et al. [31] evaluated the future changes of surface wind speed over China based on 24 GCMs from CMIP6 under three scenarios, SSP1-2.6, SSP2-4.5, and SSP5-8.5. Previous studies contributed to a thorough evaluation of both the wind resource and wind power potential in China.

However, there are few studies combining wind resource potential and characteristics with land-use suitability as well as climate change in China. Hence, there is limited awareness of the potential and features of wind power generation in the most suitable area. Furthermore, the potential effects of climate change on both the capacity and characteristics of wind resources in regions with varying suitability grades remain unexplored. This study attempts to answer the following key questions.

(1) What is the potential and suitability of onshore wind energy development across China, including its temporal characteristics?
(2) How will climate change influence the potential and spatiotemporal characteristics of wind power in areas with different suitability grades?

These issues are of significant importance for investors in project site selection and investment risk decisions, as well as for the government in achieving sustainable development. Table 1 outlines the main differences between this study and other relevant studies in China.

3. Data and climate change simulation

Due to the spatial and temporal sampling limitations of observations from meteorological stations, reanalysis data is extensively utilized as a valuable alternative. So far, various reanalysis products are accessible, with commonly used ones including ERA-Interim, REA5, and MERRA-2 [8]. The work of Hdidouan and Staffell [24] presented a summary of publicly available reanalysis datasets along with the key parameters for wind power synthesis. In this study, hourly wind speed data was extracted from the MERRA2 dataset, featuring a spatial resolution of $0.5^\circ \times 0.625^\circ$, covering the period from 1990 to 2019.

While GCMs, initially developed in the late 1950s and early 1960s, are acknowledged as effective tools for replicating large-scale circulation features of the present climate, their output is compromised in terms of resolution and accuracy [37]. Subsequently, diverse attempts have been made to simulate climate change at regional and finer spatial scales. For this purpose, this study employed multiple sets of GCM data, including HadCM3 QUMPs, ECHAM5, and HadGEM2-ES, as boundary and initial conditions to drive the PRECIS regional climate model. This facilitated the completion of dynamic downscaling simulations and predictions at a 25 km resolution within the geographical scope of China. Additional details and verification of the modeling process can be found in our previous works [38–40]. This paper specifically focuses on extracting wind speed data under the RCP 4.5 and PCP 8.5 scenarios for the late 21st century (2070–2099).

The landcover data is obtained through remote sensing from the ZY-3 Satellite, encompassing 10 main categories and 59 subcategories. Elevation and slope are derived from the 30-m resolution digital elevation model available at https://dwtkns.com/srtm30m/. The socioeconomic development levels and energy supply-demand situations of each province are sourced from the local statistical yearbooks. In the process of geospatialization, the social-economic data at the provincial level is allocated to the grid within its respective county unit. Both the MERRA2 grid and the climate change projection grid are resampled to 3 km resolution using the nearest neighbor method to match the high-resolution land-use grid to maximize the comprehensive utilization of these datasets.

4. Methodology

Fig. 1 presents the research framework of this study. It involves three main steps: land-use suitability assessment, potential and temporal characteristic evaluation, and impact analysis of future climate change. Fig. 2 illustrates the flowchart for implementing. The specific content and approaches for each step are detailed in the sub-sections.

4.1. Wind power potential estimation

This study estimates the onshore wind power potential from different perspectives, including theoretical, technical, and economic potential.

(1) Theoretical potential

The theoretical potential of wind energy is independent of the wind turbine types, usually measured by wind speed and wind power density (WPD). Near-surface wind speed can be extrapolated to a specific height by using extrapolation techniques, including the power-law [37] and log-law [41] methods. In this case, the power-law approach is adopted to project the wind speed at the desired height [5]:

$$v_w = v_m \left(\frac{h_w}{h_m} \right)^{\alpha} \tag{1}$$

where, v_w represents the wind speed at the desired height, here 110 m; v_m are corresponds to the wind speed at reference height. α is the wind shear exponent, which is related to atmospheric stability and is typically

Table 1
Summary of existing empirical studies on wind sources or wind power generation assessments for China.

Studies	Potentials			Temporal variability	Climate change	Data sources	Spatial resolution	Scope	Hub height of wind turbine	Land use or spatial constraints	Wind regime constraints	Land suitability assessment
	Resource	Technical	Economic									
[25]	✓	✓	✓	/	/	Quik SCAT ocean wind L2B12	1 km × 1 km	Offshore wind	90 m, 105 m, 120 m	✓		
[26]	✓	✓	/	✓	/	200 chosen locations (2001–2010)	provincial-scale	Onshore and offshore	100 m	✓	wind speed ≥6 m/s	
[32]	✓		✓	✓	/	6 wind measurement towers	6 selected location	Onshore	70 m			
[33]	✓			✓	/	MERRA-2 dataset (1998–2017)	50 km × 50 km		80 m, 100 m, 150 m			
[34]	✓	✓	✓	✓		MERRA-2 dataset (1980–2009)	0.625° × 0.5°	Onshore	80 m	✓		✓
[35]	✓	✓	✓		/	CFSR global atmosphere data	0.5° × 0.5°	Onshore	100 m	✓		✓
[28]	✓			✓	RCP8.5 (2025–2049 and 2075–2099)	CORDEX multi-model ensemble; Compared with the in-situ data from oceanic buoys and ERA5 database	0.44° × 0.44°	Offshore	120 m		WS < 28 m/s	
[36]	✓	✓			RCP 2.6 and RCP 8.5 (2030–2060)	CORDEX regionally downscaled climate simulations	0.44° × 0.44°	Onshore and offshore	100 m			
[29]	✓			✓	RCP 8.5 (2021–2050)	11 regional climate models (10 CORDEX models and PRECIS)	0.44° × 0.44° or 0.22° × 0.22°	Onshore	80 m			
[27]	✓	✓				CMA WRF simulation (1995–2016)	3 km × 3 km	Onshore and offshore	100 m	✓	utilization hour ≥1800 h	✓
[30]	✓			✓	SSP1-2.6, SSP2-4.5, SSP3-7.0, and SSP5-8.5.	29 CMIP5 models and 42 CMIP6 models	1° × 1°	Onshore	80 m			
This work	✓	✓	✓	✓	RCP 4.5 & RCP 8.5 (1990–2019 vs. 2070–2099)		3 km × 3 km	Onshore	110 m	✓	wind speed ≥6 m/s	✓

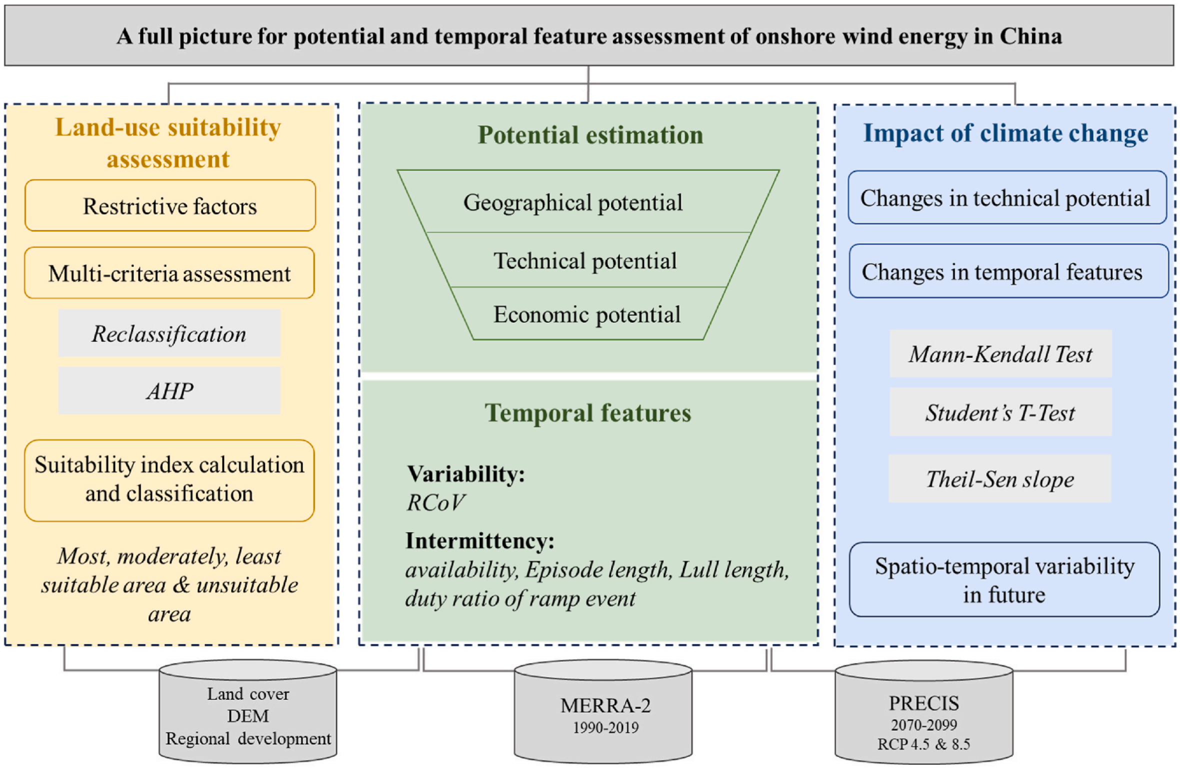

Fig. 1. The research framework of this study.

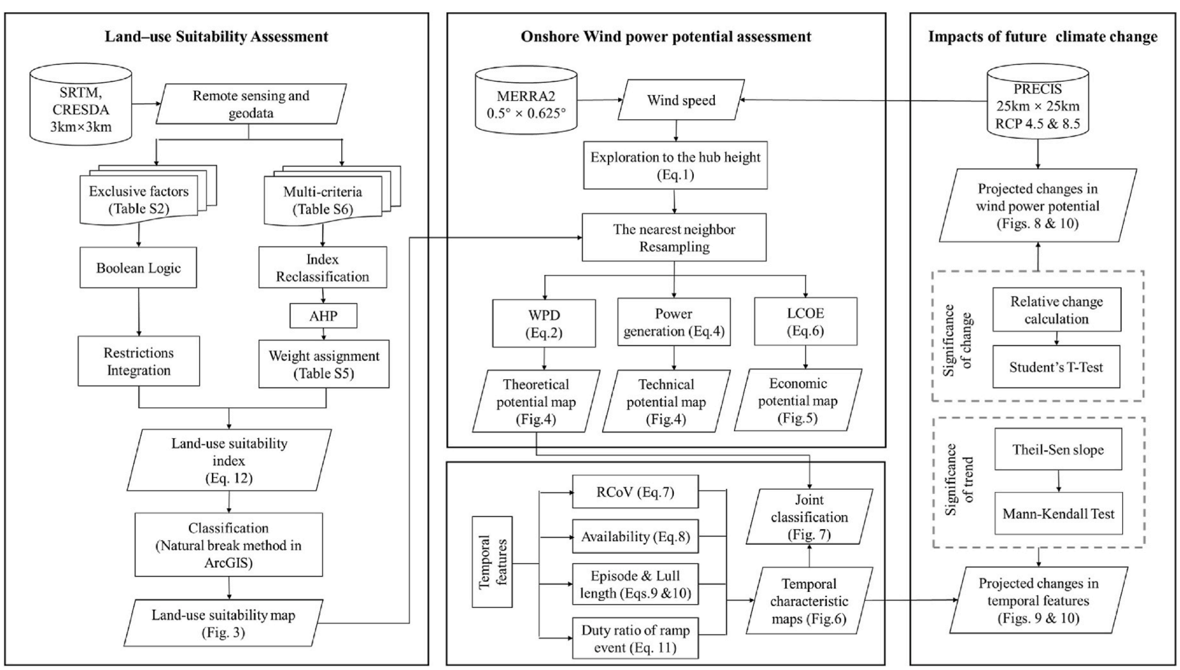

Fig. 2. The flow chart for implementing.

taken as 1/7 [28].

Wind power density assesses power per unit area, and is widely employed for quantifying the availability of wind resources, as expressed by Eq. (2) [19].

$$WPD = \frac{1}{2}\rho v_w^3 \tag{2}$$

where, ρ represents the air density, and is 1.225 kg/m^3 at 288.15 K and 1000 hPa [9,34].

(2) Technical potential

Technical potential represents the quantity of electrical energy that can be generated by a certain wind turbine type, converting the theoretical potential into useable electricity. Each wind turbine unit has a specific power curve, and the generation output varies with wind speed

[34]. Given its extensive market penetration and broad adaptability to various wind speeds [42], this study employs the Goldwind GWH191–6.0 MW unit to assess the conversion from wind speed to wind power output. Key parameters are outlined in Table S1, the power curve is obtained from the manufacturer. The output power curve of the turbine is described by Eq. (3) [35]:

$$P(v_w) = P_r \bullet \begin{cases} 0 & v_w < v_c \\ \dfrac{v_w^3 - v_c^3}{v_r^3 - v_c^3} & v_c \le v_w \le v_r \\ 1 & v_r \le v_w \le v_f \\ 0 & v_w \ge v_f \end{cases} \tag{3}$$

where, P_r is the rated power of wind turbine (MW); v_w, v_c, v_r, v_f are the actual wind, cut-in, rated, and cut-out wind speed (m/s), respectively.

In addition to the hub height and technical features of the wind turbines themselves, the layout of wind turbines significantly influences the energy production of a wind farm, mainly due to the wake effects caused by the dense distribution of turbines [43]. The longer the distance between wind turbines, the weaker the wake effects. However, this will increase the cost of integrating wind power into the grid [44]. According to existing studies, if the distance between wind turbines is 10d in the downwind direction and 3d in the crosswind direction (where d is the rotor diameter), array losses can be reduced to less than 10 % [44,45]. For the selected wind turbine in this study, GWH191–6.0 MW with a rotor diameter of 191 m, the capacity density varies with the slope in the range of 0–5.5 MW/km^2 [26]. Land-use factors for different land cover and the capacity conversion index with different slope conditions are provided in Tables S2 and S3, respectively. The technical potential is estimated as Eq. (4) [46]:

$$TP_i = 8760 \times D_i \times sf_i \times A_i \times CF_i \times \eta_{av} \times (1 - \eta_{loss}) \tag{4}$$

where, D_i is the capacity density; sf_i denotes the land use factor of grid i; A_i is the available area for wind farms, CF_i is the capacity factor; η_{av} represents the utilization efficiency of the wind turbine, here 97 %; η_{loss} denotes the comprehensive loss rate of wind farms resulting from wake effects, transmission, and other unavoidable losses, set at 15 % [45].

Capacity factor (CF), within the 0–100 % range, represents the ratio of the actual wind power output for a certain period to the maximum energy output at continuous full-power operation during the same period [5]. It usually serves as a performance indicator to compare various sites for renewable energy installation and is calculated as:

$$CF = \frac{EP}{P_r \times T} \tag{5}$$

where, EP is the total power generation during the period; T is the number of hours in the period.

(3) Economic potential

Economic potential measures that can be realized economically, for example, the levelized cost of energy (LCOE). It measures the average net present cost of electricity supplied by a power plant throughout its life cycle and is usually taken as an economic indicator for the comparison of various energy technologies. It is calculated as Eq. (6) [5]:

$$\text{LCOE} = \frac{I + \sum_{t=1}^{LT} \frac{OM_t \times EP_t}{(1+r)^t}}{\sum_{t=1}^{LT} \frac{E_t}{(1+r)^t}} \tag{6}$$

where, LT is the lifetime of the technology; I denotes the initial construction cost; OM_t is the operation and maintenance cost; EP_t is the generated electricity, and r is the discount rate. In this study, the initial construction cost and the operation and maintenance cost are set as 846 \$/kW and 0.015 \$/kWh based on the survey of large-scale onshore wind farms constructed in recent years. Lifetime is considered to be 20 years [44], and the discount rate, set at a constant 5 %, remains unchanged throughout the lifetime [13].

4.2. Temporal characteristics of wind power generation

Since the wind resource is easily affected by dynamic meteorological conditions, unstable energy output from wind farms threatens the safety and economic operation of the power grid. Thus, it is also necessary to evaluate the intermittency and variability of wind power generation.

(1) Variability

The range, standard deviation, and variance are commonly used indices to measure the variation characteristic of time series. In this study, the variability in wind resources is expressed through the relative coefficient of variation (RCoV). RCoV can be calculated concerning the mean or median, however, choosing the latter minimizes the impact of extreme values (long tails). It is calculated as [47]:

$$RCoV = \frac{median(absolute\ deviation\ about\ the\ median)}{median} \tag{7}$$

A reduced RCoV signifies less variability, indicating the high feasibility of the resource at the site. In cases where two locations exhibit identical absolute deviation about the median, the area with a greater median wind power density yields a lower RCoV value, suggesting a superior wind resource.

(2) Intermittency

Intermittency refers to the high sensitivity of wind resources to climate and weather conditions, causing wind power to fluctuate between "available" and "unavailable" states [47]. The intrinsic intermittency of wind energy would lead to intractable operation problems such as low system reliability and high reserve cost. Several indexes have been proposed to describe the intermittency [48]. This paper quantifies the intermittency through availability, episode length and lulls, and the duty ratio of ramp events.

Firstly, availability is defined as the percentage of hours in the time series where WPD exceeds a specified threshold [49], measuring the reliability or occurrences of efficient resources for power generation.

$$Availability = \frac{Number\ of\ hours\ with\ WPD \ge WPD_{th}}{Total\ number\ of\ hours} \tag{8}$$

where, WPD_{th} is the threshold of power density, here set as 200 W/m^2 [50].

The episode length refers to the duration of continuous wind power supply, serving as a crucial metric for the persistence of the wind resources [47]. Similarly, the lulls refer to the consecutive hours of almost no power generation, indicating the demand for complementary and backup energy sources [49]. The episode length and lulls of wind energy can be computed as:

$$EL = \text{Consecutive number of hours with } WPD \ge WPD_{th} \tag{9}$$

$$LL = \text{Consecutive number of hours with } WPD < WPD_{th} \tag{10}$$

According to the definition, the episode length and lull indicators only concern the intermittent when the wind speed is small. Thus, the duty ratio of ramp events, considering both a positive ramp (increase in wind resource) and a negative ramp (decrease in resource), is proposed as a complementary metric. It is calculated as [33]:

$$\lambda = T_R \times 100\% / T \tag{11}$$

where, λ represents the duty ratio of ramp events; T is the observation period; T_R is the duration of ramp events during the observation period. A ramp event occurs when the amplitude of variation in WPD at a specified time interval (e.g. 1 h) excesses a predefined threshold (e.g. 100 W/m^2).

4.3. Land-use suitability assessment for wind power deployment

Under the multi-criteria decision-making framework, the map depicting land-use suitability for wind power deployment in China is generated by considering twelve restrictive factors and three conflicting evaluation criteria.

(1) Exclusive factors

Restrictive factors should be first defined to screen out unsuitable areas. Among them, wind resource condition usually wind speed or wind power density is a primary factor to filter areas lack of economic feasibility. In this study, the minimum threshold of wind speed at 6 m/s is considered. Moreover, other constraint factors for wind farms are determined by considering topographic conditions, land cover, protected area, and transport infrastructures. Based on the previous studies and expert opinions [18,51–53], twelve restrictions for wind power plant construction are defined. An appropriate buffer is constructed for each restriction layer as specified in Table S4.

(2) Multi-criteria assessment

The power of the MCDM approach is leveraged to integrate various information and judgments regarding conflicting criteria. In this study, three main criteria (i.e. technical, economic, social, and environmental criteria) and ten sub-criteria are considered. The hierarchical comprehensive criteria system is shown in Table S5, and a detailed explanation for each criterion is presented in SI. Moreover, the MCDM method also requires assigning the weights of criteria to reflect the importance of a criterion compared to other criteria. The AHP approach, widely used in the site selection issues of energy facilities, is adopted in this study. According to this approach, the weights are objectively determined through the pairwise comparison matrix, which is constructed based on the judgments from specialists in this field [54]. The detailed process of the AHP approach can be referred to in the work of [55].

In this work, technical criteria are considered the most important factors, with the weight assigned as 0.5936, followed by social and environmental criteria (0.2493) and economic criteria (0.1571). The sub-criteria also have different important degrees for each criterion. Table S6 shows the reclassification of alternatives for each sub-criteria. Then, suitability ranking for each alternative is determined by calculating a final score through a weighted linear combination technique, as shown in Eq. (8).

$$LSI = \sum_i w_i k_i \prod_j c_j \tag{12}$$

where, LSI is the land-use suitability index for wind farms; w_i is the weight of criterion i; k_i is the score for criteria i; c_j is a binary variable, if the grid cell belongs to restricted factor j, c_j is 0; otherwise, c_j is 1. Moreover, according to the LSI, land can be divided into different classifications. Here, the restricted areas are defined as unsuitable, and other areas are classified as most, moderately, and least suitable areas by using the natural breakpoint method in ArcGIS.

4.4. Tendency analysis

The impact of climate change on onshore wind resources is characterized by calculating the changes from the baseline period (1990–2019) to the end of this century (2070–2099). In this study, the Student's t-test is applied to quantify the significance of future change. When $p < 0.05$, the null hypothesis would be rejected [24]. Moreover, the Mann-Kendall trend test, which is insensitive to outliers in time series, is also employed to examine the statistical significance of long-term trends at the grid cell level. Additionally, the Theil-Sen slope estimator is utilized to determine the magnitude of the trend, known for its improved accuracy compared to simple linear regression [56].

5. Results and discussion

In this section, the land-use suitability assessment for wind power deployment in China is first provided to highlight the most suitable areas. Then, the theoretical, technical, and economic potentials of wind power for areas with different suitability grades are presented. The temporal characteristics are also quantified by introducing statistical indicators. Finally, the impacts of future climate change are investigated to provide insights into energy planning from a long-term perspective.

5.1. Land-use suitability assessment for wind power deployment

Fig. 3 illustrates the spatial distribution of wind resources and land-use suitability assessment for wind power development. By combining the elevation map shown in Figure S1, it is found that hindered by the Himalayas, Hengduan, and Taihang Mountains, the spatial distribution of wind speed shows a distinct decreasing trend from northwest to southeast, and higher values in coastal areas compared to inland areas. The highest wind speed values (>9.0 m/s) are found in the west of the Tibetan Plateau and the east of the Inner Mongolian Plateau. Mean wind speed values lower than 6 m/s mainly occur near the Sichuan Basin in the southwest of China. In coastal areas, the wind speed (>8.0 m/s) can be found in the eastern parts of Shandong and Shanghai. Furthermore, wind resources in the southwest, the intersection of Yunnan, Guizhou, and Guangxi provinces, are also relatively abundant. Fig. 3(b) displays the spatial distribution of available areas for wind farms. It shows that the southeast of the Heihe-Tengchong Line has limited locations for wind farm deployment due to the dense population, farmland, forest, wetland, and protected area. The land-use suitability assessment map for wind farms is presented in Fig. 3(c). Suitable areas are divided into three classes, i.e. most, moderately, and least suitable, and the rest are unsuitable areas covering 65.4 % of the national territorial area. It highlights that Inner Mongolia, Xinjiang, and coastal areas are the most suitable regions for wind farms considering abundant wind resources, land-use type, economics, as well as social and environmental factors. Supplementary Table S7 presents the aggregated province-level statistics for the land-use suitability assessment.

5.2. Wind power potential assessment

Fig. 4(a) presents the spatial distribution of the theoretical potential of wind energy in terms of annual average WPD. Similar to Fig. 3(a), there is a pattern of higher wind power density in the northwest and coastal regions compared to the southwestern inland areas. The highest WPD values (>450 W/m^2) are found in the Turpan Basin of Xinjiang, a typical inland wind reservoir in China. Regions such as the Qinghai-Tibet Plateau, eastern Inner Mongolia, and northern Gansu are enriched in wind resources in China, especially large contiguous areas with WPD ranging from 300 W/m^2 to 500 W/m^2. Furthermore, coastal areas such as Jiangsu, Zhejiang, Shandong, and others also have tremendous wind resource potential. Due to the interception of the Himalayas and the Hengduan Mountains, the Yunnan-Guizhou Plateau and the Sichuan Basin in the southwest experience a rapid decrease in wind resources (WPD <100 W/m^2). Due to rugged topography and extensive forest coverage, low WPD values also occur in the Lesser Khingan Mountains and the foothills of Changbai Mountains in the northeast, as well as Wuyi Mountains in the southeast.

Figure S2 presents the seasonal pattern of wind resources in China. It shows that the Tibet Plateau and Inner Mongolia with rich wind

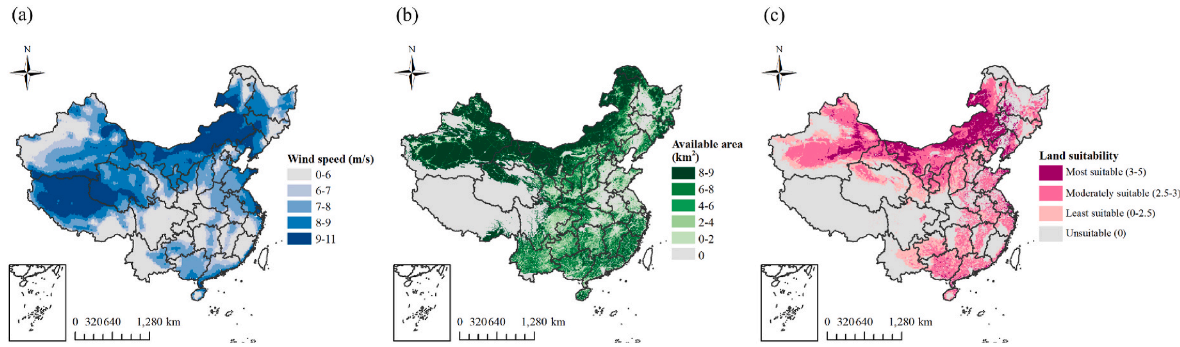

Fig. 3. Spatial distribution of wind resources and land-use suitability assessment. (a) average wind speed; (b) available area for wind power; (c) land-use suitability assessment for wind power.

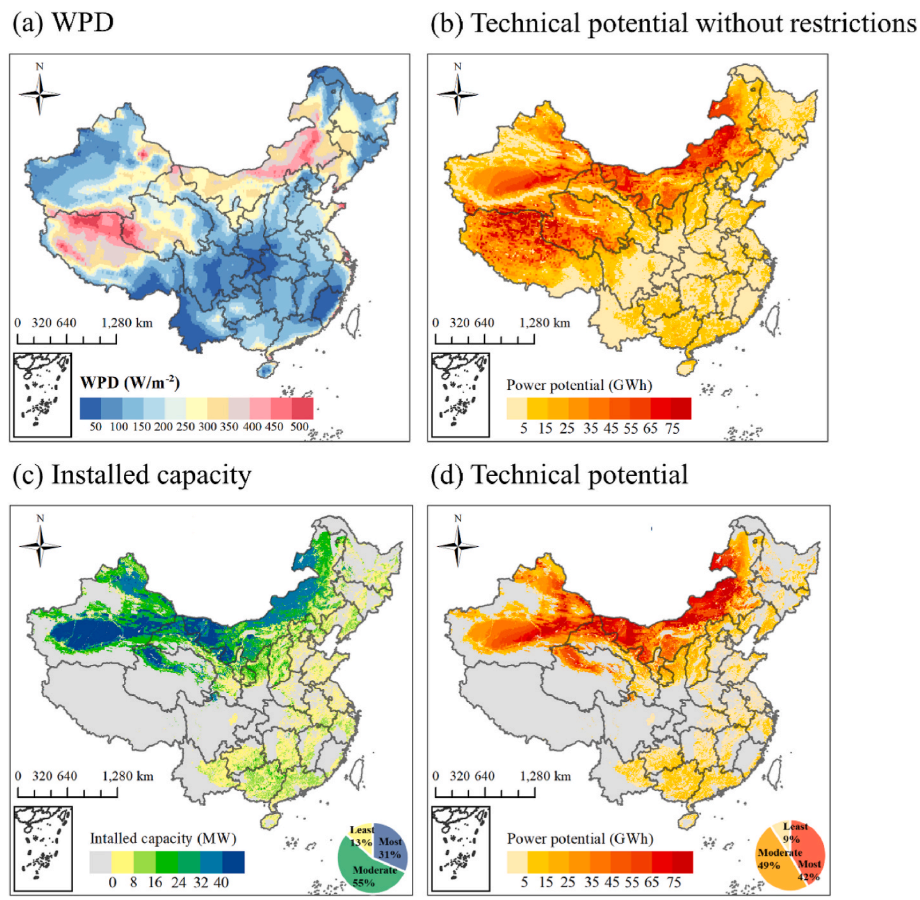

Fig. 4. Theoretical and technical potentials of wind energy in China. (a) wind power density; (b) generation potential without restrictions; (c) installed capacity potential; (b) technical generation potential. Gray indicates restricted areas.

resources will experience stronger wind variability and higher WPD in winter and spring. In winter, the highest value (WPD> 500 W/m^2) can be found in the Kunlun Mountains, the Himalayas, and the Qinghai-Tibet Plateau region with elevation greater than 4000 m. In spring, the WPD near the Turpan Basin is significantly higher than in surrounding areas. This is mainly due to the enhanced radiation within the basin, resulting in local thermal low pressure and leading to intense air convection with the surrounding areas. In comparison, the southeast monsoon from the Pacific Ocean is relatively weak in summer. Additionally, there are continuous hills along the southeastern coast extending from the coastline to the inland. Influenced by surface roughness, the intensity of wind resources rapidly diminishes. Therefore, during the summer, most parts in the south and east experience a scarcity of wind resources (WPD <150 W/m^2).

Considering the geographical constraints and land conversion coefficient, the estimated capacity potential of wind farms in China amounts to 9.6 TW, surpassing the national total installed power capacity in 2020 by five times. The corresponding annual wind power generation is up to 12.6 PWh, approximately 1.6 times the total national electricity demand (7.5 PWh). Moreover, deploying wind power projects in the most suitable areas could support 69 % (5257.4 TWh) of the national electricity consumption. Fig. 4(b)–(d) illustrate the geographical distribution of both the capacity and generation potential of wind power in China. The provincial aggregations are reported in Tables S8 and S9. It can be observed that there is a significant regional imbalance in onshore wind power installation potential. Nearly 86 % of technical potentials are concentrated in the “Three North” regions (Northwest, North China, and Northeast). Inner Mongolia, Xinjiang, and Gansu rank as the top three in terms of power generation potential (exceeding 1000 TWh) and their available area for wind power projects accounts for 63.8 % of the national geographic potential. Despite the abundance of theoretical potential, the Tibetan Plateau is not suitable for large-scale wind power deployment due to its high elevation (>3500 m). The maturation of high-altitude wind turbine technology in the future may bring opportunities to realize the transformation from theoretical potential to practice. In addition, the electricity consumption of the eastern regions accounts for 46 % of the national demand, however, the wind power potential of these areas is only 5 % of the total. Overall, the onshore wind potential and the electricity demand exhibit an inverse spatial distribution. Therefore, it is necessary to optimize the layout of renewable energy development to balance the contradictions between its production and consumption.

Fig. 5(a) displays the LCOE of wind power for each grid cell based on the given turbine type. The national average LCOE of wind power is 52.5 $/MWh, lower than the cost of traditional coal-fired power generation (60 $/MWh, regarded as the cost threshold in this study). Fig. 5(b) indicates that approximately 8.5 TW wind capacity (83 % of total potential) lies below the cost threshold, with a cost-competitive advantage in power supply. The result means that wind power has great opportunities to reduce China’s huge fossil fuel electricity consumption. Considering that local government plays an important role in the strategic planning of energy, Fig. 5(c) provides the average LCOE of wind power at the province level, varying from 37.5 $/MWh to 97.5 $/MWh. Most provinces have a competitive advantage in wind power development for grid parity. A higher wind power density implies a lower LCOE. The lowest LCOE is found in Inner Mongolia, 24 $/MWh. In economically developed regions with high population density and electricity consumption, Central and Southeast China (except for some coastal areas), the LCOE is mostly higher than 60 $/MWh. Characterized by complex terrain and scare wind resources, the average LCOE for the southwest region (covering Sichuan, Chongqing, and Yunnan provinces) is more than 90 $/MWh, and the highest value may be up to 135 $/MWh at the grid cell level. Fig. 5(d) illustrates the variation of LCOE with changes in WPD for areas with different suitability grades. For the least suitable areas, the range of LCOE varies significantly, particularly when the WPD value is low. For instance, when the WPD value is about 80 W/m^2, the LCOE ranges from 40 $/MWh to 120 $/MWh. However, as WPD increases, the LCOE decreases rapidly. For some areas with moderate suitability, even with a relatively low WPD (<120 W/m^2), they can still achieve a cost-competitive advantage benefiting from geographical advantages such as gentle slopes. For the areas with the most suitability, despite the wide range of WPD variations, nearly all grids exhibit a competitive cost advantage.

However, it should be noticed that the LCOE is a traditional and simple metric used to evaluate the techno-economic performance of wind energy and compare the competitiveness of various generation technologies. It fails to reflect the full cost that different energy sources provide to the power grid, for example, ancillary service cost caused by intermittency and insufficient flexibility, and long-distance transmission cost due to the inverse distribution of supply and demand. Moreover, it cannot capture other key performance metrics including, but not limited to, sustainability (e.g. lifecycle environmental impacts) [57], social acceptability, and macro-economic benefits (e.g. created jobs and gross value added) [58]. In some recent studies, new metrics that go “Beyond LCOE” have been proposed to better reflect the full value and costs of different energy sources from a broader systemic perspective [59]. China’s wind resource potential is enormous; however, developing more comprehensive and robust metrics may be challenging to avoid “one--size-fits-all” solutions.

5.3. Temporal features of wind power generation

Fig. 6 presents the temporal features of wind power generation under the baseline scenario. Regions with a higher RCoV, indicating greater variability in wind resources, are mainly located in the West, especially in the areas near the Kunlun, Himalayas, and Hengduan Mountains, as well as the east of Inner Mongolia (RCoV >0.75). In the eastern and central of China, the fluctuation amplitude of wind resources is

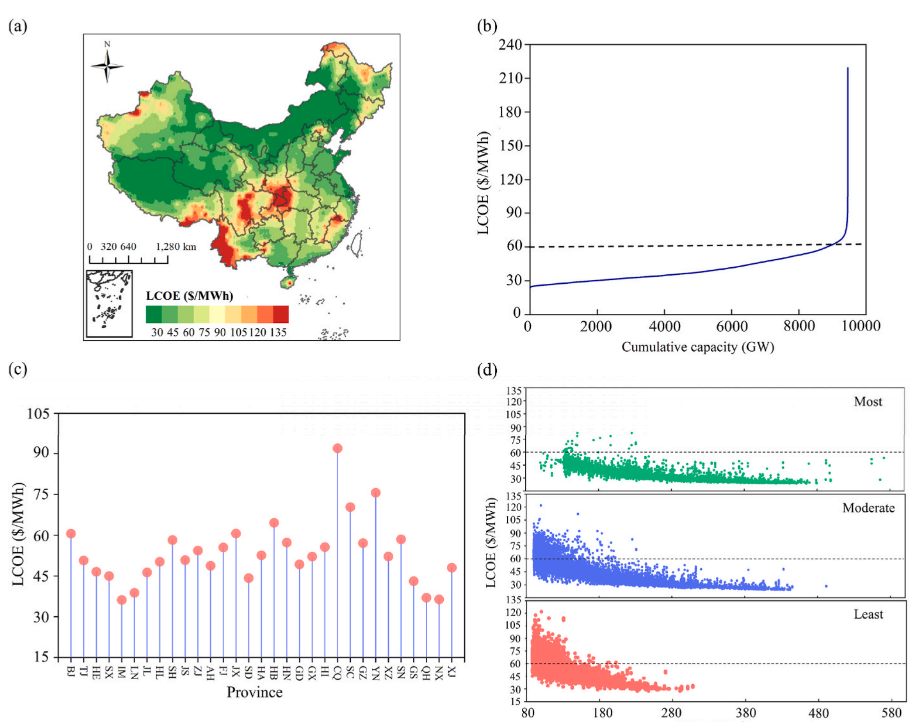

Fig. 5. LCOE and economic potential of wind power in China. (a) the special distribution of LCOE; (b) the marginal cost-supply curve of wind capacity; (c) the average LCOE at the province level; (d) the scatter plot of LCOE concerning WPD for different land-use suitability classes.

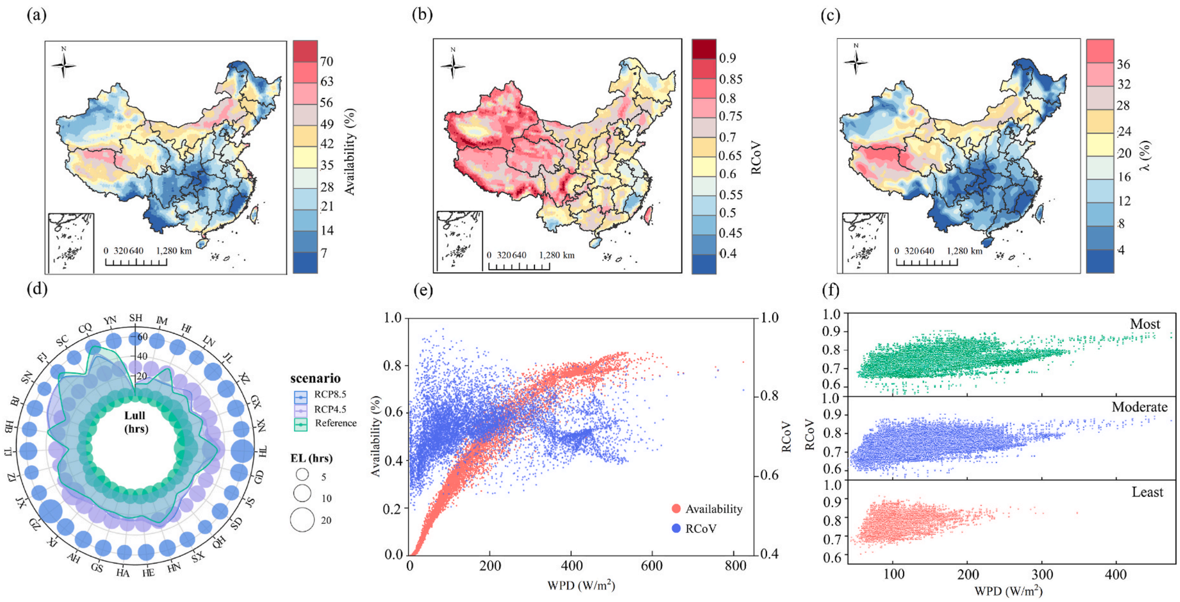

Fig. 6. Temporal features of wind power generation in China. (a) availability; (b) RCoV; (c) duty ratio of ramp event; (d) episode length and lulls; (e) the effect of WPD on availability; (f) the effect of WPD on the RCoV for grids with different suitability grades. Note: in Future 5(d), the circle represents the episode length, and the inner curve represents the lulls; green for the baseline, purple and blue for RCP 4.5 and 8.5 scenarios, respectively.

relatively small, ranging from 0.6 to 0.7. The lowest RCoV is in the Yangtze River's middle and lower plains, the Lesser Khingan Range in the northeast, and the Wuyi Mountains in the south (RCoV <0.6), indicating a relatively stable but limited wind resource. This spatial distribution is closely related to a "three-tiered" topography characteristic, a "higher in the west, lower in the east" pattern. The west of China is mainly composed of plateaus, basins, and mountains, while the eastern parts consist mainly of plains and hills. As the elevation decreases, the RCoV value gradually decreases. Figures S3 (a)–(d) and Figures S4 (a)-(d) provide the seasonal intermittency features of wind resources. The results show that the seasonal spatial distribution is consistent with the yearly pattern, where the western regions have higher values than the central and eastern regions. Wind power generation exhibits the greatest variability in spring. During spring, there is a pronounced fluctuation in wind power throughout almost the entire western region, while in other seasons, it is primarily concentrated near the mountains in the west. In autumn and winter, the overall fluctuation amplitude of wind resources decreases nationwide, especially in the south where wind resources are very stable.

Availability, EL, LL, and λ are indicators to evaluate the intermittency of wind resources. Fig. 6(e) shows the effect of WPD on availability. It is found that the availability of wind resources is positively correlated with wind power density, and regions with higher WPD tend to have longer continuous availability. Setting 200 W/m^2 as the threshold of WPD, it can be observed that the annual availability of onshore wind resources in most areas of China is greater than 21 %. The annual availability of wind resources in the Kunlun Mountains and Inner Mongolia can reach up to 70 %. Due to the influence of monsoons, wind energy resources exhibit a clear seasonal cycle, and the spatial distribution follows a similar pattern. Overall, spring and winter have higher wind resource availability, while summer and autumn have lower levels of availability. This result is consistent with a previous study [60]. The highest availability throughout the year is in winter, near the Kunlun Mountains in the west and the Greater Khingan Range in the northeast (up to 76 %). In spring, the availability in nearly half of the national territory can exceed 40 %. However, during the summer, availability is lower in most parts of the country, with 30 % of regions falling below 20 %, and the lowest availability occurring in the Hengduan Mountains, Sichuan Basin, Wuyi Mountains, Lesser Khingan Range, and Changbai Mountains, where availability ranges from 0 to 7%.

As to the duty ratio of ramp events, the highest λ value is also found in the areas near the Kunlun Mountains, exceeding 32 %. Following are the east of Inner Mongolia, the north of Gansu and Qinghai, with λ in the range of 24 %–30 %. These areas have abundant wind resources (high WPD values), whereas they also exhibit great variability (relatively high RCoV), and the average continuous availability duration is short (only 8–14 h), leading to higher electricity regulation costs. In contrast, the northeast, central, and east regions mostly have λ values lower than 12 %, implying more stable wind resources. However, these areas generally have smaller WPD values, longer durations of continuous unavailability (LL values can reach up to 40 h), and lower overall availability.

Furthermore, through a joint classification of the WPD and the RCoV index, the relationship between wind resource richness and stability is further investigated. Fig. 7 reveals that in the Northeast and below the Heihe-Tengchong Line, wind resources are limited but stability is relatively high. In contrast, the Northwest region except the Tarim basin has abundant wind resources, whereas in some areas, stability is lower (i.e. WPD >250 W/m^2 and RCoV >0.75). Furthermore, in most areas of Inner Mongolia and some areas of Tibet, both wind resources and stability are high. Fig. 6(f) also provides the relationship between RCoV and WPD for grids with different suitability grades. For grids with different suitability levels, the main difference in wind resource conditions is richness rather than stability. Moreover, it is found that a low wind generation potential is neither a necessary nor a sufficient condition for attaining high stability.

5.4. *Spatial and temporal variability under climate change*

Fig. 8 presents the projected variations in annual wind power density and technical potential by the end of this century under RCP 4.5 and RCP 8.5 scenarios. Climate change scenarios anticipate important changes in WPD by the end of the century. The downscaled climate change results indicate that regions with abundant wind resources will experience a significant decline, including Inner Mongolia and the Qinghai-Tibet Plateau. Meanwhile, there is a noticeable increase in regions with relatively scarce wind resources, mainly basins, and forests in the northeast, and hilly areas in the South. Compared to the theoretical potential, the changes in technical potential are relatively weak, and the

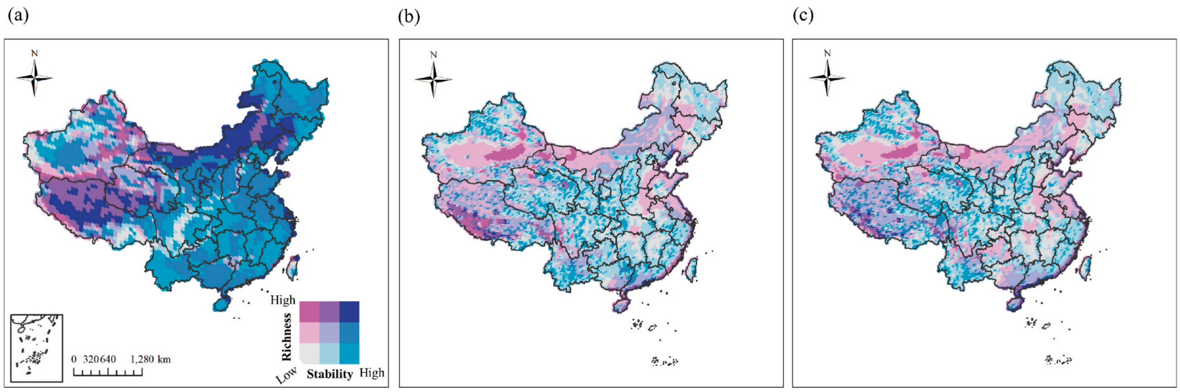

Fig. 7. The joint classification of abundance and stability of wind power under the baseline scenario (a) and future climate change scenarios RCP4.5 (b) and RCP 8.5 (c).

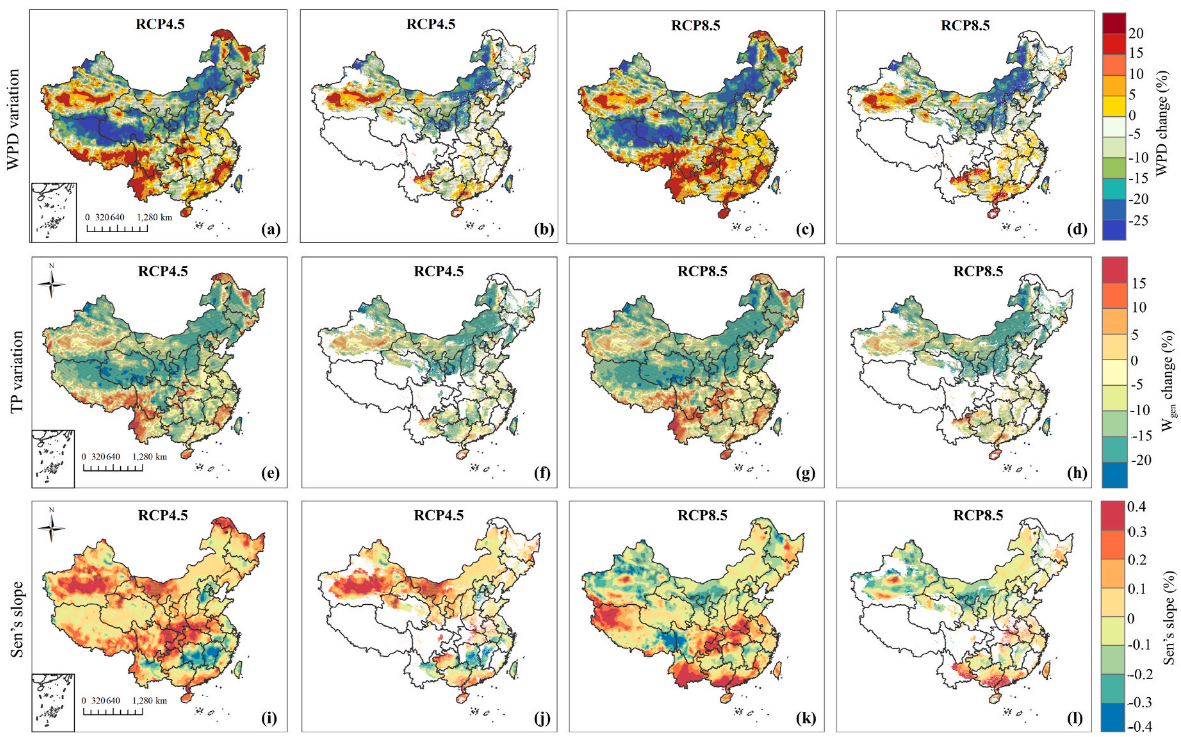

Fig. 8. Variations in wind power density and technical potential by the end of this century under different climate change scenarios. Black "√" marked areas indicate significant changes and white areas are restricted zones.

spatial pattern maintains strong similarity. Taking the RCP8.5 scenario as an example, a significant decrease is observed in most northern regions, with an average decline of up to −18 % in Inner Mongolia, Shanxi, Ningxia, and Gansu. A slight decrease is found in the Yangtze River middle and lower plains (around −5%). In the southwest and near the Tarim Basin in Xinjiang, wind power generation will experience an average increase of 7 %.

The seasonal variations of wind power density and technical potential are visualized in Figures S2(e)–(t) and S5. A remarkable generalized drop in wind power density is projected in winter in latitudes greater than 32°N. The decline also occurs in the Qinghai-Tibet Plateau and Inner Mongolia in spring and autumn. However, in summer, the wind power density shows an increasing trend across the entire nation. The patterns of change in wind power, both seasonally and spatially, exhibit a notable consistency across various emission scenarios. Under the RCP8.5 scenario, the overall change trend is consistent with the RCP4.5 scenario, with the main difference being an increased decline in WPD in the northern part of Inner Mongolia and an enhanced increase in the Chongqing-Guizhou region. Moreover, climate projections in this scenario present more intensive seasonal variations and differences. In winter, the WPD presents a well-spread drop of ~25 % surrounding the Kunlun Mountains, Helan Mountains, Yinshan Mountains, and Taihang Mountains. On the contrary, significant rises in wind power density are anticipated during the summer.

Overlaying the land-use restriction layer with the WPD and technical potential variation maps, it is found that the areas with significant changes in wind resources are mostly within restricted zones (except for the Tarim Basin in Xinjiang and Inner Mongolia), which are areas lacking technical feasibility. In addition, although the future wind resource in the southwest is expected to increase, implying a positive influence, the overall contribution can be negligible due to limited the available land resources for development. Thus, the national technical potential of onshore wind power shows a declining trend in the future, decreasing by −27.3 % and −29.5 % under RCP4.5 and RCP8.5

scenarios. The technical potential experiences the greatest reduction in winter, decreasing by −34.1 % (756.1 TWh) and −38.6 % (855.9 TWh) for RCP 4.5 and 8.5 scenarios; while in summer it is projected to increase by 3 % (72.7 TWh) and 6 % (145.5 TWh). The aggregated variations at the provincial level are reported in Table S10.

Fig. 9 illustrates the changes in volatility and intermittency characteristics of wind power across the country under climate change. Given the positive correlation between availability and WPD, the changes in the availability at both the annual and seasonal scales are generally consistent with the variations in the WPD under climate change scenarios. In most regions, availability may decrease, with significant reductions in the Kunlun Mountains, Loess Plateau, and Inner Mongolia Plateau (<−15 %). Correspondingly, the duration of continuous unavailability of wind resources in Tibet and Qinghai will increase. Availability in the Tarim Basin of Xinjiang, the Himalayan Mountains, and the southwestern region of the Yunnan-Guizhou Plateau shows a noticeable upward trend (>10 %). In these areas, the continuous availability duration in Xinjiang and Yunnan will also increase to varying degrees. Changes in other regions are relatively small. This trend is further strengthened under the RCP8.5 scenario. The future trends and spatial distribution characteristics of the duty ratio of ramp events are highly consistent with availability. Compared with Fig. 6, regions with higher RCoV under the baseline scenario show an improvement in wind resource volatility, while areas with lower RCoV values experience a deterioration in future wind resource stability. In the future, RCoV in the East, Northeast, South, and the Tarim Basin in Xinjiang will increase. Specifically, increases of up to 20 % are predicted in the Tarim Basin under the RCP 4.5 scenario. In the wind-rich Inner Mongolia region, most of the eastern areas are expected to experience a slight increase in RCoV (within 15 %), while other areas show a smaller range of RCoV changes (less than 5 %). However, some wind-rich areas also see an improvement in stability; RCoV in the Qinghai-Tibet Plateau, Yunnan-Guizhou Plateau, and northern Xinjiang are projected to decrease, with a range of −10 % to −25 %. Except for the Lesser Khingan Mountains, and a few areas in Yunnan and Fujian, the duty ratio of ramp events is expected to improve nationwide. Similarly, Figures S3 (e)–(t) and S4 (e)-(t) illustrate the seasonal variations in wind resource stability and intermittency features under future climate change. The variations in these indicators across seasons are consistent with the annual trends. By overlaying the land-use restricted layer, it can be observed that the availability and λ values of most available lands will decrease, while RCoV values increase. In summary, influenced by climate change, the abundance of wind resources decreases, overall instability increases, but abrupt events decrease.

The joint classification in Fig. 7(b) and (c) provide a more intuitive change trend in wind resource characteristics, both the abundance and stability of wind resources in China show an overall downward trend. The most significant decline can be observed in Qinghai-Tibet Plateau and Inner Mongolia, followed by Xin Jiang and eastern coastal areas where wind resources have increased as volatility has creased. The WPD in the Yangtze River middle and lower reaches plain shows little change (within the range of −5%–5 %); however, the RCoV is expected to significantly increase, up to 15 %. In the Himalayan Mountains and Yunnan region, WPD will increase, and overall RCoV is expected to decrease, indicating an improvement in wind resource conditions. However, the overall pattern of wind resource conditions in China remains relatively stable, with Inner Mongolia, the northwest part of Tibet, and coastal areas continuing to exhibit the best comprehensive performance in terms of abundance and stability.

Fig. 10 illustrates the distribution of projected changes in wind energy potentials and temporal features for land with different suitability grades under climate change. In general, the variation of each indicator for different suitability grades follows a normal distribution. There is little difference in the distribution of WPD among different grades. For each suitability grade, more than 75 % of the grid cells experience an increase in WPD during the summer. The range of variation in WPD in other seasons is greater than that in the summer. In comparison, the technical potential for different suitable land grades is showing a declining trend. Among them, the decline is more pronounced in the most suitable areas, and the range of variations is more concentrated.

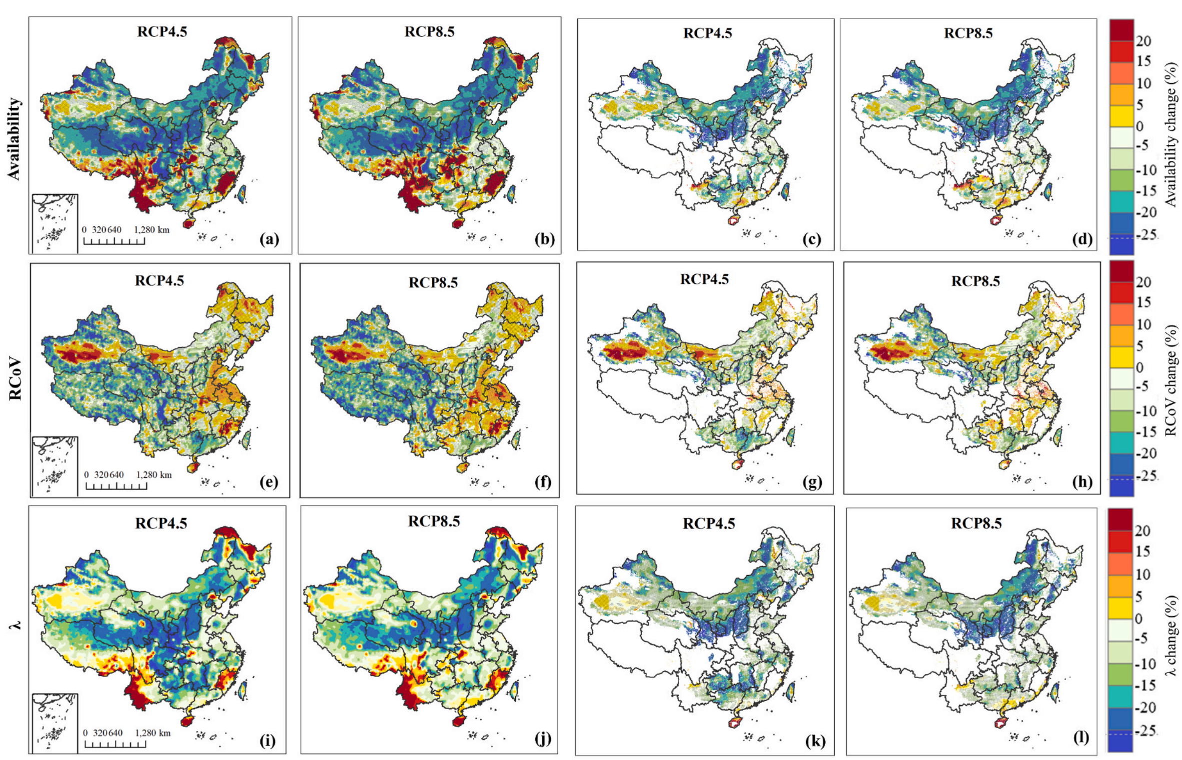

Fig. 9. The changes in temporal characteristics of wind power under RCP 4.5 and 8.5 scenarios. The area covered by "√" signifies regions with significant changes, while the white area denotes restricted zones.

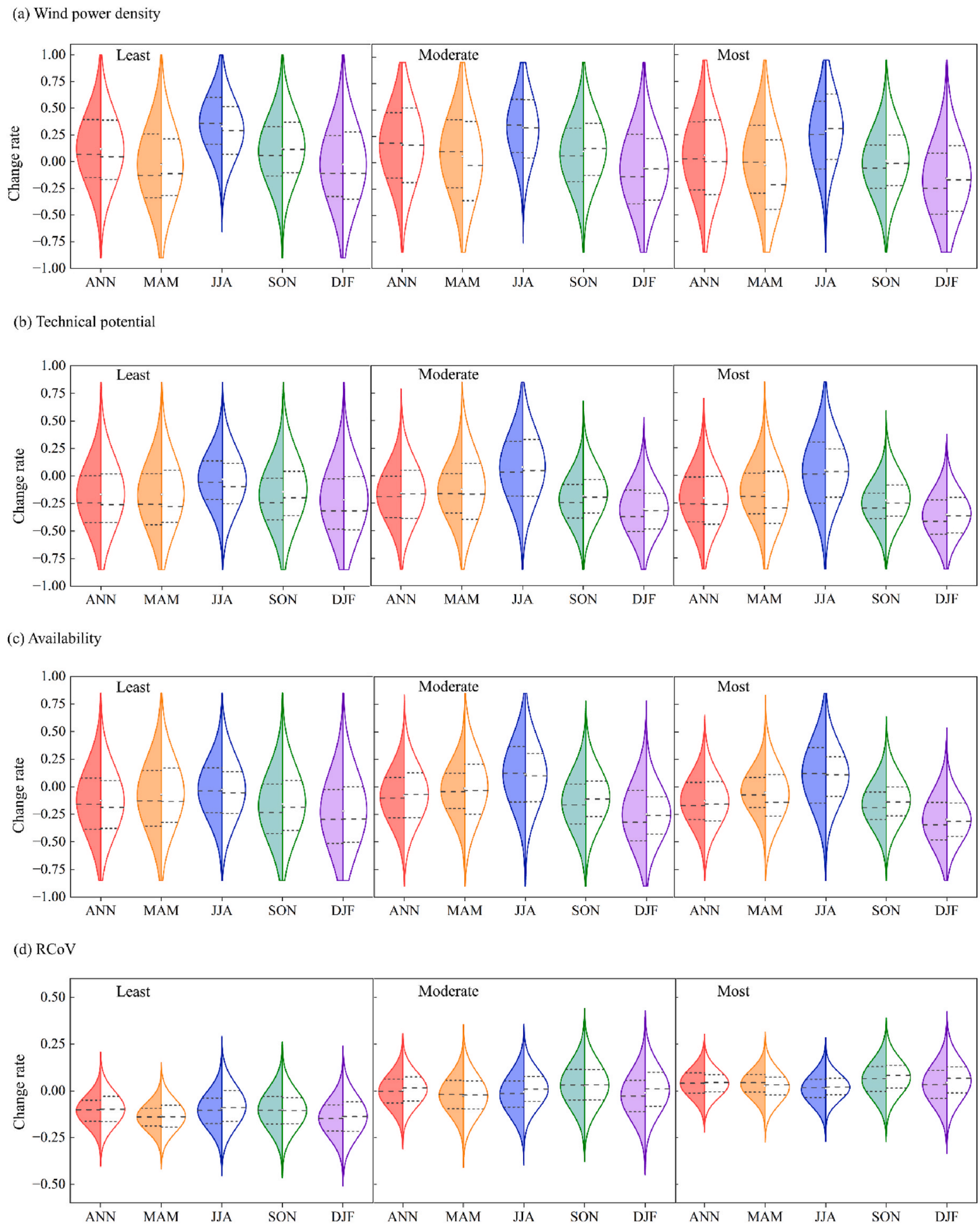

Fig. 10. Distribution of projected changes in wind resources and temporal features under the different climate change scenarios. (a) WPD, (b) technical potential, (c) availability, (d) RCoV. The left and right side of the violin corresponds to RCP 4.5 and RCP 8.5 scenarios. The horizontal width shows the value distribution of overall grid points, and the wider regions highlight more grid cells that have this value. The dashed lines from top to bottom represent the upper quartile, median, and lower quartile, respectively.

The distribution of availability changes is consistent with the technical potential. The distribution of projected changes in RCoV is relatively concentrated, and there are significant differences among different suitability grades. In the most suitable areas, nearly 75 % of the grids have an increase in RCoV value. For the moderately suitable level, the grids show an equal distribution of increased and decreased RCoV values. In the least suitable areas, over 75 % of the grids exhibit a decrease in RCoV value, indicating an improvement in wind resource stability. Additionally, compared to other suitability levels, the most suitable areas have the smallest range of changes at annual and seasonal scales, with a relatively concentrated distribution and fewer outliers. However, for a certain suitability grade, there is a significant variation in RCoV changes in winter. By comparing the left and right sides of the violin plots, the difference in variations of projected changes in wind resources and temporal features for the different climate change scenarios is roughly the same, with more extreme values in the projections under the RCP8.5 scenario.

5.5. Comparison with existing research and uncertainties

This sector compares the results of this study with other existing research and discusses the potential uncertainties by focusing on the section on wind turbines and the allocation of criteria priority.

(1) Comparison with existing research

Numerous prior studies have offered potential estimates for wind energy in China, employing various assumptions regarding land suitability and exclusion criteria. For example, the work of He and Kammen [26] estimated 0.83 TW (lower case)/1.81 TW (upper case) wind capacity potential with 1.24 TWh (lower case)/2.64 TWh (upper case) power generation output. However, it only reports the provincial scale potential estimation and rough temporal variation. Table S11 presents a comparison of the assessment results in this study with other recent research outcomes. The results in this study are relatively close to those of [31] but higher than those of [37]. The reasons for such differences stem from various factors, including the adopted meteorological database, the covered study period, the considered geographical constraints (e.g. altitude, slope), the selected wind turbine types, and the assumed turbine layout.

Moreover, the overall conclusions regarding the impacts of climate change also align with previous studies. The work of Monforti et al. [38] projected a decline in the capacity factor of wind energy in North China, particularly in Inner Mongolia during spring, summer, and fall. However, it primarily focused on China and India, considering the RCP 2.6 and RCP 8.5 scenarios, with relatively low temporal and spatial resolution. In addition to the wind power potential assessment, this study focuses on evaluating the suitability of land for wind power deployment. It compares the technical potential, economic feasibility, and temporal characteristics of wind power deployed in areas with different suitability levels, as well as the impact of climate change. The key findings serve as a basis for nationwide decision-making on the organized development of wind power and grid integration.

(2) Impacts of wind turbine selection

For the robustness analysis of technical potential assessment, another type of wind turbine, GWH 204-5.6 MW with a larger swept area and more suitable for medium or low wind speed areas, is selected for comparison. By adopting this technique, the threshold of wind speed limitation could be 5 m/s, as a result, the available area would increase by 4 %. Especially in areas with scarce wind resources, such as Central and South China, the technical potential for wind power increases significantly, with an average increase of over 20 %. This indicates that advancements in wind turbine technology will bring more opportunities for wind power deployment. In addition, these areas are densely populated and economically developed, with high electricity demand. Utilizing local wind resources can enhance energy self-sufficiency and avoid energy losses associated with long-distance transmission. Furthermore, the deployment of turbines with larger swept areas results in a more dispersed layout, leading to a reduction in capacity density and the estimated total installed capacity (8.05 TW, 17 % lower than the GWH 191-6.0 MW technology). However, the superior performance of the new wind turbine, characterized by lower specific power but a higher capacity factor, will lead to an increase in total electricity generation (5.2 PWh, an increase of 41 %). Meanwhile, it is also noteworthy that the optimized layout of large-scale wind farms could also contribute to improved landscape aesthetic quality and greater public acceptance.

Considering future climate change, wind resources are projected to decrease in the west and north, and increase in the south. The adoption of new wind power conversion technology will significantly mitigate the decline in wind power potential, especially in the least suitable area, where the reduction is about −15 %. This indicates that more efficient, low-wind-speed-adapted turbines can alleviate the negative impacts of climate change on wind power development to some extent. Figure S6 illustrates the estimated technical potential for areas with different suitability grades by adopting different wind turbines. The results indicate a significant increase in the technical potential of the least suitable area, with an increase of 0.28 PWh (about 48 %). The impact on the potential evaluation of moderate and most suitable areas is less pronounced. Under the RCP 4.5 scenario, although the total power generation with the new technology decreases, it remains comparable to the total amount under the GWH 191-6.0 MW technology in the baseline scenario.

(3) Impacts of criteria weight allocation

To check the robustness of the evaluation results, sensitivity analysis is usually conducted to reveal the effect on the rankings of alternatives by changing the priority weights of sub-criteria. Some studies applied the same weights for all criteria; some others removed some specific criteria for comparison [55]. The results of [61] indicate that the change in the criteria weights will influence the rank of the alternatives. Thus, sensitivity analysis is also performed to provide more insights. Four extra scenarios are defined and described in Table S12, which are equal weight (Scenario 1), economic priority (Scenario 2), socio-environment priority (Scenario 3), and technical priority (Scenario 4). The land suitability evaluation results are presented in Table S13.

It is found that except for the original scenario and the economically prioritized scenario (Scenario 2), the area classified as the most suitable land is relatively high, almost or exceeding 50 %. Notably, under the socially and environmentally prioritized criteria (Scenario 3), 77.3 % of the available land is classified as the most suitable, indicating that most of the available land has favorable environmental development conditions. In contrast, under the economically prioritized scenario (Scenario 2), only 12.5 % of the available land is deemed most suitable. This suggests that although there is a vast amount of available land, the economic feasibility of wind energy development is low for most areas due to limitations in current energy infrastructure and the long distance from electricity demand centers. Overall, the classification results under the original scenario precisely identify priority development areas while comprehensively considering multi-criteria trade-offs, providing effective guidelines for strategic planning.

6. Conclusions

In this study, a thorough assessment of onshore wind energy in China is performed with a 3 km spatial resolution. By considering several conflicting criteria, land-use suitability assessment for wind power deployment is characterized by different classes. It can serve for national-scale power system planning and site selection of wind farm projects. Given the significance of addressing the operational challenges associated with intermittent wind energy, the analysis of temporal features aids in identifying areas with low/high stability of wind power. This analysis also assists in evaluating the need for flexibility resources. Lastly, this study explores the impacts of climate change on wind power potential along with its temporal features for available areas with different suitability classes. The primary findings of this study can be summarized as follows:

The total available area for onshore wind farms accounts for 34.6 % of the country, and the most suitable areas are in the North (27.8 %). The capacity potential of onshore wind in China is 9.6 TW with 12.6 PWh annual power generation. Based on the levelized cost analysis, the economic potential will be 8.5 TW (83 % of the total technical potential). Especially the east of Inner Mongolia has the lowest levelized cost of energy, 24 $/MWh. Highly suitable areas for wind energy are inversely distributed with developed economies and dense populations, indicating that long-distance power transmission is necessary to achieve optimal resource allocation. However, regions abundant in wind resources exhibit greater variability and intermittency, implying higher electricity regulation costs. The effective utilization of wind resources will promote advancements and investments in ultra-high voltage transmission technologies as well as energy storage technologies to regulate power quality and ensure grid security.

Influenced by climate change, over 75 % of grid cells within the most suitable areas is an observed decline in wind energy. While a noticeable enhancement is projected in the least suitable areas. From a seasonal perspective, a significant overall decrease is forecasted during winter in latitudes greater than 32°N; and a slight upward trend across the entire nation during summer. The national technical potential of onshore wind power is projected to decrease by 27.3 % and 29.5 % under RCP 4.5 and RCP 8.5 scenarios. Under the RCP 4.5 scenario, the technical potential for wind power in most and moderate suitable areas will decrease by 32.2 % (1.7 PWh) and 23.0 % (1.4 PWh), respectively. Additionally, a decline in wind resources could lead to fewer ramp events. It contributes to enhanced grid stability and reduction in maintenance costs for wind power infrastructure, potentially extending its operational lifespan. Furthermore, the smoother power output patterns resulting from a decreased intermittency enable more effective utilization of energy storage resources.

However, it needs to be emphasized that wind power potential estimation is significantly related to wind turbine technology and land use. The judgments of decision-makers will have a great influence on the results when selecting the geospatial limits and evaluation criteria and determining their weights. Therefore, the application of sensitivity analysis of weights may contribute to the authenticity and robustness of the results. Moreover, the use of the MERRA database and extrapolation techniques as a proxy of actual measured data is another source of uncertainty. It is challenging to appropriately handle bias correction introduced by climate projections, especially for regions with complex orography. The robustness of the projection should be further discussed by comparing different models. To offer a more comprehensive understanding of future climate scenarios, it is essential to consider future projections of wind speed under some more complex climate change scenarios such as SSPs. Therefore, the outcomes presented in this study should be regarded as an initial representation of potential assessment, temporal-spatial variability, and future trends of wind energy in China. It is expected to be combined with energy system planning models, providing a foundation for policymakers to formulate appropriate regulations and policies for the effective integration of renewable energy. The research framework proposed in this study could be future-tailored and expanded for other areas to support wind energy planning with regard to climate change and energy security.

CRediT authorship contribution statement

Ling Ji: Conceptualization, Formal analysis, Writing – original draft, Funding acquisition. **Jiahui Li:** Methodology, Visualization, Formal analysis, Writing – original draft. **Lijian Sun:** Visualization, Software. **Shuai Wang:** Investigation, Conceptualization. **Junhong Guo:** Software, Validation. **Yulei Xie:** Writing – review & editing. **Xander Wang:** Supervision, Writing – review & editing.

Declaration of competing interest

The authors declare that they have no known competing financial interests or personal relationships that could have appeared to influence the work reported in this paper.

Data availability

Data will be made available on request.

Acknowledgments

This work was supported by the Beijing Nova Program (No. 20220484034), and the National Natural Science Foundation of China (No. 52379001, No. 72074013, and No. 52222901). We highly acknowledge the NASA Earth Data officials for the data availability.

Appendix A. Supplementary data

Supplementary data to this article can be found online at https://doi.org/10.1016/j.rser.2024.114778.

References

[1] Energy Institute (EI). Statistical review of world energy. London, UK: EI; 2023.
[2] National Energy Administration. 2022 national power industry statistics. https://www.nea.gov.cn/2023-01/18/c_1310691509.htm (accessed February 20, 2024).
[3] Electric Power Planning and Engineering Institute (EPPEI). China electricity development report. Beijing, China: China Daily; 2023.
[4] Bandoc G, Prăvălie R, Patriche C, Degeratu M. Spatial assessment of wind power potential at global scale. A geographical approach. J Clean Prod 2018;200:1065–86. https://doi.org/10.1016/j.jclepro.2018.07.288.
[5] Jain A, Das P, Yamujala S, Bhakar R, Mathur J. Resource potential and variability assessment of solar and wind energy in India. Energy 2020;211:118993. https://doi.org/10.1016/j.energy.2020.118993.
[6] McElroy MB, Lu X, Nielsen CP, Wang Y. Potential for wind-generated electricity in China. Science 2009;325:1378–80. https://doi.org/10.1126/science.1175706.
[7] Fazelpour F, Markarian E, Soltani N. Wind energy potential and economic assessment of four locations in Sistan and Balouchestan province in Iran. Renew Energy 2017;109:646–67. https://doi.org/10.1016/j.renene.2017.03.072.
[8] Nezhad MM, Neshat M, Groppi D, Marzialetti P, Heydari A, Sylaios G, et al. A primary offshore wind farm site assessment using reanalysis data: a case study for Samothraki island. Renew Energy 2021;172:667–79. https://doi.org/10.1016/j.renene.2021.03.045.
[9] Jung C, Schindler D, Laible J. National and global wind resource assessment under six wind turbine installation scenarios. Energy Convers Manag 2018;156:403–15. https://doi.org/10.1016/j.enconman.2017.11.059.
[10] Enevoldsen P, Permien F-H, Bakhtaoui I, Krauland A-K von, Jacobson MZ, Xydis G, et al. How much wind power potential does europe have? Examining european wind power potential with an enhanced socio-technical atlas. Energy Pol 2019;132:1092–100. https://doi.org/10.1016/j.enpol.2019.06.064.
[11] Mattar C, Guzmán-Ibarra MC. A techno-economic assessment of offshore wind energy in Chile. Energy 2017;133:191–205. https://doi.org/10.1016/j.energy.2017.05.099.
[12] Lopez A, Mai T, Lantz E, Harrison-Atlas D, Williams T, Maclaurin G. Land use and turbine technology influences on wind potential in the United States. Energy 2021;223:120044. https://doi.org/10.1016/j.energy.2021.120044.
[13] Rinne E, Holttinen H, Kiviluoma J, Rissanen S. Effects of turbine technology and land use on wind power resource potential. Nat Energy 2018;3:494–500. https://doi.org/10.1038/s41560-018-0137-9.
[14] Silva Herran D, Dai H, Fujimori S, Masui T. Global assessment of onshore wind power resources considering the distance to urban areas. Energy Pol 2016;91:75–86. https://doi.org/10.1016/j.enpol.2015.12.024.
[15] Elkadeem MR, Younes A, Mazzeo D, Jurasz J, Elia Campana P, Sharshir SW, et al. Geospatial-assisted multi-criterion analysis of solar and wind power geographical-technical-economic potential assessment. Appl Energy 2022;322:119532. https://doi.org/10.1016/j.apenergy.2022.119532.
[16] Shorabeh SN, Firozjaei HK, Firozjaei MK, Jelokhani-Niaraki M, Homaee M, Nematollahi O. The site selection of wind energy power plant using GIS-multi-criteria evaluation from economic perspectives. Renew Sustain Energy Rev 2022;168:112778. https://doi.org/10.1016/j.rser.2022.112778.
[17] Ali S, Taweekun J, Techato K, Waewsak J, Gyawali S. GIS based site suitability assessment for wind and solar farms in Songkhla, Thailand. Renew Energy 2019;132:1360–72. https://doi.org/10.1016/j.renene.2018.09.035.
[18] Konstantinos I, Georgios T, Garyfalos A. A Decision Support System methodology for selecting wind farm installation locations using AHP and TOPSIS: case study in Eastern Macedonia and Thrace region, Greece. Energy Pol 2019;132:232–46. https://doi.org/10.1016/j.enpol.2019.05.020.
[19] Chen L. Impacts of climate change on wind resources over North America based on NA-CORDEX. Renew Energy 2020;153:1428–38. https://doi.org/10.1016/j.renene.2020.02.090.
[20] Solaun K, Cerdá E. Impacts of climate change on wind energy power – four wind farms in Spain. Renew Energy 2020;145:1306–16. https://doi.org/10.1016/j.renene.2019.06.129.
[21] Carvalho D, Rocha A, Gómez-Gesteira M, Silva Santos C. Potential impacts of climate change on European wind energy resource under the CMIP5 future climate projections. Renew Energy 2017;101:29–40. https://doi.org/10.1016/j.renene.2016.08.036.
[22] Russo MA, Carvalho D, Martins N, Monteiro A. Future perspectives for wind and solar electricity production under high-resolution climate change scenarios. J Clean Prod 2023;404:136997. https://doi.org/10.1016/j.jclepro.2023.136997.

[23] He JY, Li QS, Chan PW, Zhao XD. Assessment of future wind resources under climate change using a multi-model and multi-method ensemble approach. Appl Energy 2023;329:120290. https://doi.org/10.1016/j.apenergy.2022.120290.

[24] Hdidouan D, Staffell I. The impact of climate change on the levelised cost of wind energy. Renew Energy 2017;101:575–92. https://doi.org/10.1016/j.renene.2016.09.003.

[25] Hong L, Möller B. Offshore wind energy potential in China: under technical, spatial and economic constraints. Energy 2011;36:4482–91. https://doi.org/10.1016/j.energy.2011.03.071.

[26] He G, Kammen DM. Where, when and how much wind is available? A provincial-scale wind resource assessment for China. Energy Pol 2014;74:116–22. https://doi.org/10.1016/j.enpol.2014.07.003.

[27] Wang Y, Chao Q, Zhao L, Chang R. Assessment of wind and photovoltaic power potential in China. Carb Neutrality 2022;1:15. https://doi.org/10.1007/s43979-022-00020-w.

[28] Costoya X, deCastro M, Carvalho D, Feng Z, Gómez-Gesteira M. Climate change impacts on the future offshore wind energy resource in China. Renew Energy 2021;175:731–47. https://doi.org/10.1016/j.renene.2021.05.001.

[29] Zhuo C, Junhong G, Wei L, Fei Z, Chan X, Zhangrong P. Changes in wind energy potential over China using a regional climate model ensemble. Renew Sustain Energy Rev 2022;159:112219. https://doi.org/10.1016/j.rser.2022.112219.

[30] Miao H, Xu H, Huang G, Yang K. Evaluation and future projections of wind energy resources over the Northern Hemisphere in CMIP5 and CMIP6 models. Renew Energy 2023;211:809–21. https://doi.org/10.1016/j.renene.2023.05.007.

[31] Wu J, Shi Y, Xu Y. Evaluation and projection of surface wind speed over China based on CMIP6 GCMs. J Geophys Res-Atmos 2020;125:e2020JD033611. https://doi.org/10.1029/2020JD033611.

[32] Li Y, Wu X-P, Li Q-S, Tee KF. Assessment of onshore wind energy potential under different geographical climate conditions in China. Energy 2018;152:498–511. https://doi.org/10.1016/j.energy.2018.03.172.

[33] Ren G, Wan J, Liu J, Yu D. Characterization of wind resource in China from a new perspective. Energy 2019;167:994–1010. https://doi.org/10.1016/j.energy.2018.11.032.

[34] Gao Y, Ma S, Wang T, Wang T, Gong Y, Peng F, et al. Assessing the wind energy potential of China in considering its variability/intermittency. Energ Convers Manage 2020;226:113580. https://doi.org/10.1016/j.enconman.2020.113580.

[35] Feng J, Feng L, Wang J, King CW. Evaluation of the onshore wind energy potential in mainland China—based on GIS modeling and EROI analysis. Resour Conserv Recycl 2020;152:104484. https://doi.org/10.1016/j.resconrec.2019.104484.

[36] Sherman P, Song S, Chen X, McElroy M. Projected changes in wind power potential over China and India in high resolution climate models. Environ Res Lett 2021;16:034057. https://doi.org/10.1088/1748-9326/abe57c.

[37] Sailor DJ, Smith M, Hart M. Climate change implications for wind power resources in the Northwest United States. Renew Energy 2008;33:2393–406. https://doi.org/10.1016/j.renene.2008.01.007.

[38] Guo J, Huang G, Wang X, Xu Y, Li Y. Projected changes in wind speed and its energy potential in China using a high-resolution regional climate model. Wind Energy 2020;23:471–85. https://doi.org/10.1002/we.2417.

[39] Guo J, Huang G, Wang X, Wu Y, Li Y, Zheng R, et al. Evaluating the added values of regional climate modeling over China at different resolutions. Sci Total Environ 2020;718:137350. https://doi.org/10.1016/j.scitotenv.2020.137350.

[40] Guo J, Wang X, Xiao C, Liu L, Wang T, Shen C. Evaluation of the temperature downscaling performance of PRECIS to the BCC-CSM2-MR model over China. Clim Dyn 2022;59:1143–59. https://doi.org/10.1007/s00382-022-06177-5.

[41] Shu ZR, Li QS, Chan PW. Statistical analysis of wind characteristics and wind energy potential in Hong Kong. Energy Convers Manag 2015;101:644–57. https://doi.org/10.1016/j.enconman.2015.05.070.

[42] Monforti F, Huld T, Bódis K, Vitali L, D'Isidoro M, Lacal-Arántegui R. Assessing complementarity of wind and solar resources for energy production in Italy. A Monte Carlo approach. Renew Energy 2014;63:576–86. https://doi.org/10.1016/j.renene.2013.10.028.

[43] Grassi S, Junghans S, Raubal M. Assessment of the wake effect on the energy production of onshore wind farms using GIS. Appl Energy 2014;136:827–37. https://doi.org/10.1016/j.apenergy.2014.05.066.

[44] Mentis D, Siyal SH, Korkovelos A, Howells M. A geospatial assessment of the techno-economic wind power potential in India using geographical restrictions. Renew Energy 2016;97:77–88. https://doi.org/10.1016/j.renene.2016.05.057.

[45] Manwell JF, McGowan JG, Rogers AL. Wind energy explained. New York: Wiley; 2009.

[46] Ferguson-Martin CJ, Hill SD. Accounting for variation in wind deployment between Canadian provinces. Energy Pol 2011;39:1647–58. https://doi.org/10.1016/j.enpol.2010.12.040.

[47] Prasad AA, Taylor RA, Kay M. Assessment of solar and wind resource synergy in Australia. Appl Energy 2017;190:354–67. https://doi.org/10.1016/j.apenergy.2016.12.135.

[48] Fant C, Gunturu B, Schlosser A. Characterizing wind power resource reliability in southern Africa. Appl Energy 2016;161:565–73. https://doi.org/10.1016/j.apenergy.2015.08.069.

[49] Gao Y, Ma S, Wang T. The impact of climate change on wind power abundance and variability in China. Energy 2019;189:116215. https://doi.org/10.1016/j.energy.2019.116215.

[50] Gunturu UB, Schlosser CA. Characterization of wind power resource in the United States. Atmos Chem Phys 2012;12:9687–702. https://doi.org/10.5194/acp-12-9687-2012.

[51] Jangid J, Bera AK, Joseph M, Singh V, Singh TP, Pradhan BK, et al. Potential zones identification for harvesting wind energy resources in desert region of India - a multi criteria evaluation approach using remote sensing and GIS. Renew Sustain Energy Rev 2016;65:1–10. https://doi.org/10.1016/j.rser.2016.06.078.

[52] Ayodele TR, Ogunjuyigbe ASO, Odigie O, Munda JL. A multi-criteria GIS based model for wind farm site selection using interval type-2 fuzzy analytic hierarchy process: the case study of Nigeria. Appl Energy 2018;228:1853–69. https://doi.org/10.1016/j.apenergy.2018.07.051.

[53] Asadi M, Ramezanzade M, Pourhossein K. A global evaluation model applied to wind power plant site selection. Appl Energy 2023;336:120840. https://doi.org/10.1016/j.apenergy.2023.120840.

[54] Saaty TL. A scaling method for priorities in hierarchical structures. J Math Psychol 1977;15:234–81. https://doi.org/10.1016/0022-2496(77)90033-5.

[55] Saraswat SK, Digalwar AK, Yadav SS, Kumar G. MCDM and GIS based modelling technique for assessment of solar and wind farm locations in India. Renew Energy 2021;169:865–84. https://doi.org/10.1016/j.renene.2021.01.056.

[56] Ji L, Wu Y, Xie Y, Sun L, Huang G. An integrated framework for feasibility analysis and optimal management of a neighborhood-scale energy system with rooftop PV and waste-to-energy technologies. Energ Sustain Dev 2022;70:78–92. https://doi.org/10.1016/j.esd.2022.07.012.

[57] Kuckshinrichs W, Koj JC. Levelized cost of energy from private and social perspectives: the case of improved alkaline water electrolysis. J Clean Prod 2018;203:619–32. https://doi.org/10.1016/j.jclepro.2018.08.232.

[58] de Andres A, MacGillivray A, Roberts O, Guanche R, Jeffrey H. Beyond LCOE: a study of ocean energy technology development and deployment attractiveness. Sustain Energy Technol Assessments 2017;19:1–16. https://doi.org/10.1016/j.seta.2016.11.001.

[59] Vanegas-Cantarero MM, Pennock S, Bloise-Thomaz T, Jeffrey H, Dickson MJ. Beyond LCOE: a multi-criteria evaluation framework for offshore renewable energy projects. Renew Sustain Energy Rev 2022;161:112307. https://doi.org/10.1016/j.rser.2022.112307.

[60] Yang L, Jiang J, Liu T, Li Y, Zhou Y, Gao X. Projections of future changes in solar radiation in China based on CMIP5 climate models. Glob Energy Inter 2018;1:452–9. https://doi.org/10.14171/j.2096-5117.gei.2018.04.005.

[61] Moradi S, Yousefi H, Noorollahi Y, Rosso D. Multi-criteria decision support system for wind farm site selection and sensitivity analysis: case study of Alborz Province, Iran. Energy Strateg Rev 2020;29:100478. https://doi.org/10.1016/j.esr.2020.100478.